Impact of heterogeneous delays on cluster synchronization

Sarika Jalan[1,2,*] and Aradhana Singh[1]

[1]*Complex Systems Lab, Indian Institute of Technology Indore, M-Block, IET-DAVV Campus, Khandwa Road, Indore 452017, India*

[2]*Centre for Bio-Science and Bio-Medical Engineering, Indian Institute of Technology Indore, M-Block, IET-DAVV Campus, Khandwa Road, Indore 452017, India*

(Received 19 April 2014; revised manuscript received 23 August 2014; published 9 October 2014)

We investigate cluster synchronization in coupled map networks in the presence of heterogeneous delays. We find that while the parity of heterogeneous delays plays a crucial role in determining the mechanism of cluster formation, the cluster synchronizability of the network gets affected by the amount of heterogeneity. In addition, heterogeneity in delays induces a rich cluster pattern as compared to homogeneous delays. The complete bipartite network stands as an extreme example of this richness, where robust ideal driven clusters observed for the undelayed and homogeneously delayed cases dismantle, yielding versatile cluster patterns as heterogeneity in the delay is introduced. We provide arguments behind this behavior using a Lyapunov function analysis. Furthermore, the interplay between the number of connections in the network and the amount of heterogeneity plays an important role in deciding the cluster formation.

DOI: 10.1103/PhysRevE.90.042907 PACS number(s): 05.45.Xt, 05.45.Pq

I. INTRODUCTION

Cluster synchronization has been investigated in many complex systems such as ecological, nervous, social, coupled semiconductor lasers, and electrical power systems [1–8]. In these systems the interactions among units are not instantaneous due to the finite speed of information transmission causing a time delay [9]. Most of the work pertaining to delays has considered a homogeneous delay [10–19], however, in real world networks the rate of information transmission from all the units may not be the same [20]. Hence, model systems incorporating heterogeneity in delays advance a more realistic framework. A few previous studies examining systems having heterogeneous delays have shown them to follow emerging behaviors as observed for homogeneous delays [21]. A recent work demonstrates that an optimal level of delay heterogeneity may maximize the stability of the uniform flow, which has implications in traffic dynamics [22]. Another recent work involving electronic circuits with heterogeneous delays demonstrates the change in cluster patterns and suppression of synchronization [23]. Furthermore, heterogeneous delays have been shown to bear a more secured communication in chaos based encryption systems [24].

In this paper we investigate the impact of heterogeneous delays on the mechanism of cluster synchronization. So far, very few studies have focused on the impact of heterogeneity in delay values on phase synchronized clusters [4,5,23,25]. In addition, attempts still need to be made to find out the mechanism behind cluster synchronization in the presence of heterogeneity in the delay values. Undelayed and homogeneously delayed coupled systems have been identified with two different mechanisms of synchronized cluster formation, namely, the driven (D) and the self-organized (SO) [6,7,14,15].

We find that a large amount of heterogeneity in delays, as defined in Sec. II, leads to better synchronizability of the underlying network, while the parity of the delay plays an important role in the mechanism of cluster formation. At weak coupling, even heterogeneous delays lead to SO clusters, odd heterogeneous delays lead to the D clusters, and even-odd heterogeneous delays lead to mixed clusters. Furthermore, we demonstrate that heterogeneous delays lead to rich cluster patterns. Cluster pattern refers to a particular state which contains information on all pairs of synchronized nodes distributed in various clusters in the network [14]. We present results for coupled chaotic maps on various networks, namely, one-dimensional (1D) lattice, small-world (SW), Erdös-Rényi (ER) random, scale-free (SF), and the complete bipartite [26]. The complete bipartite networks, which have been known to form robust ideal D clusters for undelayed and homogeneous delayed evolution [7,8,14], yield different cluster patterns upon the introduction of heterogeneity in the delays.

The paper is organized as follows. We describe the model along with definitions of (phase) synchronization and (phase) synchronized clusters in Sec. II. Thereafter, Sec. III presents numerical results for coupled dynamics on all the networks. Section IV discusses an analytical understanding of the observed results using complete bipartite networks. We discuss the effect of the change in the amount of heterogeneity in delays on the phase synchronized clusters in Sec. V, followed by the results for the coupled circle maps in Sec. VI. In addition, Sec. VII studies the effect of the Gaussian distributed delays on the phase synchronized clusters. We also present the effect of average degree on the cluster synchronization in Sec. VII, and discuss the results with conclusions and future directions in the last section.

II. MODEL: COUPLED MAPS WITH HETEROGENEOUS DELAYS

We consider a network of N nodes and N_c connections between the nodes. Let each node of the network be assigned a dynamical variable x_i, $i = 1,2,\ldots,N$. The dynamical evolution is defined by the well known coupled

*sarika@iiti.ac.in

maps [9,27]

$$x_i(t+1) = (1-\varepsilon) f(x_i(t)) + \frac{\varepsilon}{\sum_{j=1}^{N} A_{ij}} \sum_{i=1}^{N} A_{ij} g(x_j(t-\tau_{ji})). \quad (1)$$

Here A is the adjacency matrix with elements A_{ij} taking values 1 and 0 depending upon whether or not there is a connection between i and j. We consider undirected networks which lead to the symmetric adjacency matrix, i.e., $A_{ij} = A_{ji}$. The delay $\tau_{ij} = \tau_{ji}$ is the time it takes for the information to reach from a unit i to its neighbor j. The function $f(x)$ defines the local nonlinear chaotic map, $g(x)$ defines the nature of coupling between the nodes, and ε is the overall coupling constant.

In the present investigation we consider networks with two types of delay arrangements: (i) two delay values and (ii) a Gaussian distributed delay. The first arrangement is achieved by randomly making a fraction of connections f_{τ_1} conducting with τ_1, and another fraction f_{τ_2} conducting with delay τ_2. These two parameters are defined as $f_{\tau_1} = N_{\tau_1}/N_c$ and $f_{\tau_2} = N_{\tau_2}/N_c$, where N_{τ_1} and N_{τ_2} stand for the number of connections with delay τ_1 and τ_2, respectively. Maximum heterogeneity is exhibited when half of the connections bear a τ_1 delay and the other half bear a τ_2 delay. We remark that these definitions do not incorporate the exact values of delay and only take care of the number of connections conducting with different delay values. We consider $h = 1 - |f_{\tau_1} - f_{\tau_2}|$ as a measure of the amount of heterogeneity in the network. The value of h being zero corresponds to homogeneous delays, whereas $h = 1$ corresponds to $f_{\tau_1} = f_{\tau_2}$, denoting maximum heterogeneity.

Also, we define the cluster synchronizability of a network in terms of the number of nodes participating in the clusters. Based on this, we say cluster synchronizability enhances if the number of nodes participating in the clusters increases in the network. Note that some of the earlier works have defined global synchronizability of the network in terms of the ratio of the maximum and the first nonzero eigenvalues of the Laplacian of a graph [28]. In the present paper our definition of the synchronizability is based on cluster synchronization.

We investigate the first arrangement of two delay values in detail and then consider a Gaussian distributed delay arrangement. Depending on the parity of the delay, we classify three types of heterogeneity: (a) odd-odd heterogeneity, (b) odd-even heterogeneity, and (c) even-even heterogeneity. We find that these three types have a distinct impact on the coupled dynamics, and hence may give rise to different patterns of clusters as well as mechanisms behind their origin. We present detailed results for the logistic map as this simple map has been used widely and has exhibited a wide range of emergent behaviors observed so far in the nonlinear dynamics [9]. We also present results for the circle maps in order to demonstrate the robustness of the observed phenomena.

Synchronized and phase synchronized clusters

Exact synchronization corresponds to a state where the dynamical variables of the nodes have identical values ($x_i = x_j, \forall t > t_0$), whereas in the case of phase synchronization the dynamical variables for the nodes have some definite relation between their phases [29–31]. Cluster synchronization corresponds to a state where some of the nodes in a network are (phase) synchronized with each other, while they are not (phase) synchronized with the rest of the nodes of the network [31]. Depending on the mechanism of cluster formation, as discussed in the Introduction, there can be SO, D, or mixed clusters [6–8,14,15,32]. In the numerical investigation presented here, we consider sparse networks, primarily in order to avoid global synchronization (as the present paper focuses on cluster synchronization) and, more importantly, to have a better understanding of the mechanisms underlying cluster synchronization. As sparse networks yield exact synchronization for very few nodes, we consider phase synchronization. The definition of the phase for the discrete dynamical system is taken from Refs. [6,33] as $d_{ij} = (1 - \nu_{ij})/\max(\nu_i, \nu_j)$, which was further proved to follow the metric properties [7]. In this expression ν_i and ν_j denote the number of times the dynamical variables $x_i(t)$ and $x_j(t)$, $t = t_0, t_{0+1}, \ldots, t_0 + T - 1$, for nodes i and j show local minima (maxima) during the time interval T starting from some time t_0, with ν_{ij} denoting the number of times local minima (maxima) match with each other. Further, $d_{ij} = d_{ji}$, and $d_{ij} = 0$ when all the minima (maxima) of the variable x_i and x_j match with each other, whereas $d_{ij} = 1$ when none of the minima (maxima) match. Thus the phase synchronization between two nodes exists if the above defined phase distance between them vanishes.

Also, we use f_{intra} and f_{inter} as the measures for intracluster and intercluster couplings [6]: $f_{\text{intra}} = N_{\text{intra}}/N_c$ and $f_{\text{inter}} = N_{\text{inter}}/N_c$, where N_{intra} and N_{inter} are the numbers of intracluster and intercluster couplings, respectively. In N_{inter}, coupling between two isolated nodes is not included. The criteria for the distinction of different cluster states are as follows [34]: The state, corresponding to $f_{\text{intra}} = 0$ and $f_{\text{inter}} > 0$, is defined as the ideal D cluster state as the mechanism behind the synchronization is intercluster couplings, and the state corresponding to $f_{\text{intra}} > 0$ and $f_{\text{inter}} \sim N_{\text{cl}}\langle k\rangle/N_c$ (N_{cl} is the number of clusters) is defined as the ideal SO cluster state as the mechanism behind the synchronization between pairs of nodes is due to intercluster couplings. Further, if $|f_{\text{intra}} - f_{\text{inter}} < th$, the clusters are of mixed type. The phase diagram is presented for $th = 0.2$. For the higher values of th, as long as $f_{\text{intra}} > f_{\text{inter}}$ ($f_{\text{intra}} < f_{\text{inter}}$), clusters are considered here to be of dominant SO (dominant D) type.

In order to further explain the cause (mechanism) and effect (synchronized clusters), which forms a backbone of the present work, we plot the schematic diagram (Fig. 1). For an ideal D cluster [for example, nodes 1 and 3 in Fig. 1(a)], there is no direct connection between the nodes, thus the synchronization

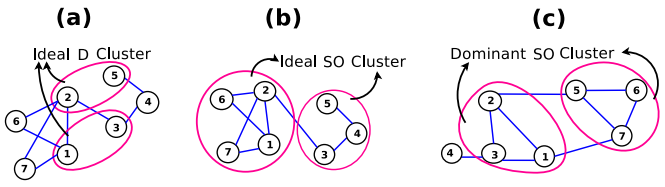

FIG. 1. (Color online) Schematic diagram depicting the (a) ideal D, (b) ideal SO, and (c) dominant SO clusters. The nodes (small solid circles) in the circular region represent that they are synchronized.

between these nodes is driven by the coupling outside the cluster, whereas for the SO cluster [Fig. 1(b), containing nodes 1, 2, 6, and 7] all the connections, except *one*, which is essential to keep the network connected, lie within the cluster, indicating that the synchronization between the pairs of nodes is due to intracluster couplings. We remark that deducing such a direct relation between the cause (mechanism) and effect (cluster synchronization) is not straightforward for the dominant SO, D, and mixed clusters. For example, in Fig. 1(c) the mechanism behind the formation of the dominant SO cluster (comprising nodes 1, 2, 3, 6, and 7) can be due to the inter- or intracouplings or due to the mixed effect of both types of couplings, however, the observation of the ideal SO and D clusters as discussed above forms a basis to define the dominant D and SO cluster states as well.

III. COUPLED MAPS WITH TWO DELAY VALUES

Starting with random initial conditions, Eq. (1) is evolved and the phase synchronized clusters for T time steps after an initial transient are studied. This paper considers diffusive coupling $[g(x_i,x_j) = g(x_j) - g(x_i)]$ because of its relevance in real world systems [9,21]. Note that the other forms of couplings, such as linear, may yield different results for the same coupling value, but key phenomena observed for diffusive couplings such as different mechanisms of cluster formation would remain the same [6,7]. In the following first we present the results for maximum heterogeneity $f_{\tau_1} = f_{\tau_2}$, followed by discussions on the impact of the amount of heterogeneity on cluster formation.

A. 1D lattice and SW networks

The 1D lattices used in the simulation have circular boundary conditions with each node having $\langle k \rangle$ nearest neighbors. Figure 2(a) plots a phase diagram depicting different cluster states based on the values of f_{inter} and f_{intra}, and Fig. 2(c) displays the fraction of nodes forming a cluster (F_{clus}) for the 1D lattice. In the absence of any coupling, all the nodes evolve independently in a chaotic manner which solely depends upon the value of the initial condition. As coupling is introduced ($\varepsilon > 0$), the coupled dynamics displays emerging behavior depending upon the delayed interactions and the strength of the coupling. With even-odd parity (say, $\tau_1 = 1$ and $\tau_2 = 2$) for very weak coupling values ($\varepsilon < 0.16$) the local chaotic dynamics dominates over the interaction terms and all the nodes keep evolving in an isolated manner. As coupling is further increased, the coupling range ($0.16 \lesssim \varepsilon \gtrsim 0.25$) leads to the mixed cluster state. As ε increases further, there is an emergence of dominant D clusters [Fig. 2(a)] leading to mixed clusters for strong couplings. For odd-odd parity, the ideal SO or dominant SO clusters are formed. The snapshots in Fig. 3(a) demonstrate the ideal SO clusters for the 1D lattice. Note that here the value of F_{clus} is *one* as all the nodes participate in the cluster formation, but they distribute in different clusters instead of forming a globally synchronized state. Hence, F_{clus} being one does not provide criteria for the globally synchronized state.

Further, the intermediate and strong couplings exhibit a manifestation of dominant D clusters. A comparison with

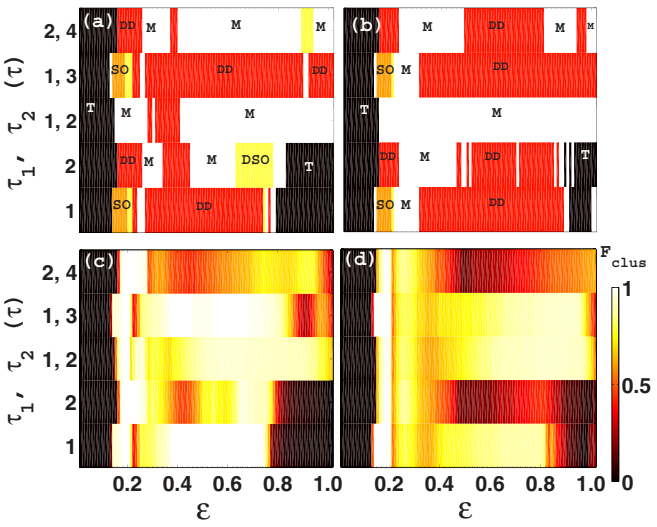

FIG. 2. (Color online) Phase diagrams (a) and (b) show different regions in the parameter space of τ_1,τ_2 (τ for homogeneous delays) and ϵ for $f(x) = 4x(1-x)$. The gray (color) denotes different regions: turbulent (T) (stands for no cluster formation), ideal driven (D), dominant driven (DD), ideal self-organized (SO), dominant self-organized (DSO), and mixed (M). In these phase diagrams, the boundaries of the ideal D and ideal SO clusters do not depend on the threshold value, while the boundaries of the dominant D, SO, and mixed clusters depend on the threshold chosen. (c) and (d) show variations in the fraction of nodes forming clusters ($F_{\text{clus}} = N_{\text{clus}}/N$, where N_{clus} = total number of nodes forming clusters) in the parameter space of τ_1,τ_2 (τ for homogeneous delays) and ε for $f(x) = 4x(1-x)$. The values on the y axis represent the delay values. Network parameters are $N = 500$ and $\langle k \rangle = 4$. The gray (color) coding represents the variation in the fraction of nodes forming clusters. (a), (c) correspond to the 1D lattice and (b), (d) correspond to the SF networks.

the homogeneous delay evolution leads to the conclusion that heterogeneous delays cause an enhancement in synchronization for strong couplings while keeping the D mechanism responsible for the cluster formation. For even-even parity, the coupled dynamics at a weak ε range manifests the formation of ideal D clusters, as observed for even homogeneous delays [Fig. 2(a)]. We remark that the definition of phase

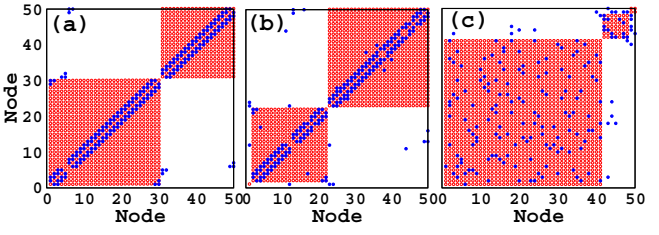

FIG. 3. (Color online) The ideal SO clusters for the (a) 1D lattice, (b) SW, and (c) random networks. Squares represent clusters, diagonal dots represent isolated nodes, while off-diagonal dots imply that the two corresponding nodes are coupled (i.e., $A_{ij} = 1$). In each case the node numbers are reorganized so that the nodes belonging to the same cluster are numbered consecutively. The example corresponds to networks with $N = 50$, $\langle k \rangle = 4$, and $\varepsilon = 0.17$. All the graphs correspond to $f_{\tau_1} = f_{\tau_2}$, $\tau_1 = 1$, and $\tau_2 = 3$.

synchronization and the phase distance used here assign antiphase synchronization (minima of one node matching with maxima of the other) into two different clusters as the phase distance for this case remains one. However, this particular situation of the nodes being antiphase synchronized [29] is not observed very often for chaotic situations (for example, Fig. 5 for $t < t_0$). With an increase in the coupling strength, at intermediate and strong couplings, mixed clusters are formed [Fig. 2(a)]. At the strong couplings where the undelayed and the homogeneous delays do not lead to cluster synchronization, for even-even heterogeneous delays, 50% of the nodes participate in cluster formation [Fig. 2(c)].

The delayed coupled maps on the SW networks, generated using the Watts-Strogatz algorithm by rewiring probability p_r [26], do not display any distinguishable changes as compared to the corresponding 1D lattice described above. Thus for 1D lattice and SW networks the mechanism behind the cluster formation depends on the parity of the delay values. At weak coupling, even heterogeneous delays are associated with the D mechanism, odd heterogeneous delays are associated with the SO mechanism, while mixed heterogeneous delays are associated with the mixed mechanism. Thus, a change in the parity of the heterogeneous delay values may give rise to a transition from one phenomenon to the other phenomenon. We provide arguments supporting this parity dependence in Sec. IV.

B. SF networks

We now turn our attention to the SF network, which has completely different structural properties [26] than the 1D lattice and the SW networks. SF networks are constructed by starting with $\langle k \rangle$ nodes and then adding one node with $\langle k \rangle$ connections at each step [26]. The weak coupling range displays a similar result as for the regular networks described in the previous section for all types of heterogeneity, whereas intermediate couplings do not display the transition from one mechanism to other, as observed for the regular networks, which exhibit a transition from the dominant SO cluster state to the dominant D cluster state and instead yield D or mixed clusters for all the parities [Fig. 2(b)]. Comparing the three heterogeneities leads to the conclusion that even-even heterogeneity in delays causes less of an enhancement in the fraction of nodes forming clusters, as compared to odd-odd and odd-even heterogeneity [Fig. 2(d)]. The phenomenon of suppression in the fraction of nodes forming clusters for a particular heterogeneity becomes more prominent with the increase in delay values. At strong couplings, odd-odd heterogeneity in delays manifests a better cluster synchronizability of SF networks as compared to the corresponding 1D lattice and SW networks [Figs. 2(c) and 2(d)].

Random networks display a better synchronization than the corresponding regular networks even for undelayed and homogeneous delays [6,10,14]. The interesting finding in the presence of heterogeneous delays is that the enhancement in the cluster synchronizability of the network may be accompanied with the nodes directly connected, as is evident from the mixed clusters in Fig. 2. We remark that D clusters were already observed for homogeneous delays in the intermediate ε range for the SF networks, indicating synchronization between nodes which are not directly connected [14], therefore the occurrence of synchronization between these nodes for high coupling ranges is not very surprising. We can fairly conclude that the SO mechanism has a major role to play in the enhancement of synchronization in the presence of heterogeneous delays, which further becomes clearly visible for the complete bipartite network. In order to understand the copious behavior observed in the dynamical evolution of regular and random networks with heterogeneous delays, we conduct an elaborate investigation for the complete bipartite networks in Sec. IV.

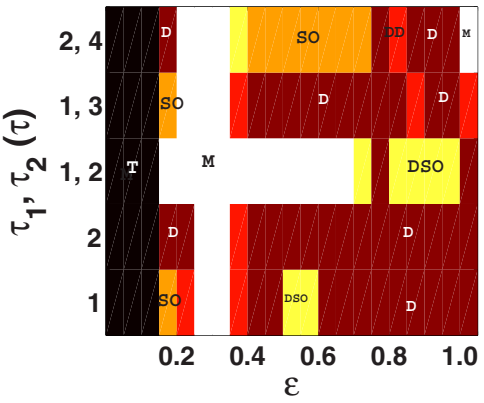

FIG. 4. (Color online) Phase diagrams (a) and (b) showing different regions in the parameter space of τ_1, τ_2 (τ for homogeneous delays) and ϵ for a complete bipartite network of $N = 500$. The figure description is the same as for Figs. 2(a) and 2(b).

C. Complete bipartite networks

Complete bipartite networks consist of two sets where all the nodes of one set (say, A) are connected with those of the second (say, B). Results are presented for both sets having an equal number of nodes. The simple structure of these networks, on one hand, makes analytical studies easier to carry, and, on the other hand, the capability of the network to yield rich cluster patterns such as ideal D, SO, and mixed clusters brings it into the same platform of the other random networks. Figure 4 plots a phase diagram depicting different cluster states based on the values of f_{inter} and f_{intra} for complete bipartite networks. Note that for the homogeneous delays themselves the coupled dynamics exhibits participation of all the nodes in the cluster formation, and the introduction of heterogeneity in the delay does not change this number. The phase diagram in Fig. 4 shows that at weak couplings, as discussed for the other networks, complete bipartite networks also exhibit ideal D clusters for even delays, while for odd delays, instead of the ideal SO cluster state as exhibited by the other networks discussed above, complete bipartite networks lead to the globally synchronized sate. We remark that complete bipartite networks do not show ideal SO clusters, as due to their topology it is not possible to divide the whole network in ideal SO clusters, however, mixed or dominant SO and D states are possible, for instance, at intermediate couplings and strong couplings where homogeneous delays lead to robust D clusters, and the heterogeneity in the delays generates D,

mixed, or dominant SO clusters depending upon the parity of the heterogeneous delays and the coupling strength [Fig. 4(a)].

IV. ANALYTICAL INSIGHT

In the following, we perform a Lyapunov function analysis in order to obtain an understanding of the destruction of the robust D clusters for homogeneous delays to different cluster states for heterogeneous delays, and present some arguments for the transition from ideal D clusters to the SO cluster state upon introduction of heterogeneity in the delays at intermediate and strong couplings.

First, we analyze the case of the transition from the D clusters to different cluster states. The Lyapunov function for a pair of nodes can be written as [6,35]

$$V_{ij}(t) = [x_i(t) - x_j(t)]^2. \tag{2}$$

$V_{ij}(t) \geqslant 0$ and the equality holds well when nodes i and j are exactly synchronized. The Lyapunov function for a pair of nodes on a complete bipartite network in the presence of heterogeneous delays, using Eqs. (1) and (2), can be written as

$$V_{ij}(t+1) = \Bigg[(1-\epsilon)[f(x_i(t)) - f(x_j(t))] + \frac{2\varepsilon}{N} \sum_{j=N/2+1}^{N} g(x_j(t-\tau_{ji})) - \frac{2\varepsilon}{N} \sum_{i=1}^{N/2} g(x_i(t-\tau_{ij})) \Bigg]^2. \tag{3}$$

Let us consider a pair of nodes of the same set having homogeneous delays, which leads to the situation where coupling terms having delay values in Eq. (3) get canceled, thereby commencing the D clusters, which are robust against the change in the delay values [14]. However, in the presence of heterogeneity in the delay values, the coupling term having delay values does not vanish in Eq. (3), and thus may or may not emulate the synchronization between these nodes depending upon the delay arrangements of these two nodes, and may be leading to nodes from the same set organizing into different clusters. Note that for parameter mismatch [36,37], the coupling term bearing the delay values does not vanish and the nodes from the same set may get distributed into different clusters even for the undelayed and homogeneously delayed cases. We remark that the Lyapunov function analysis performed here for the complete bipartite network works for clusters having exactly synchronized nodes (see Fig. 5).

Furthermore, we remark that for the undelayed and homogeneously delayed cases, the nodes receiving the same input can be considered as forming a set (say, A in Fig. 6), similar to the complete bipartite networks, and the nodes which are giving the same inputs to these can be considered to form another set (say, B in Fig. 6). The synchronization criteria for nodes in set A depend on whether or not these nodes are directly connected.

For the first case, when the nodes in set A are not directly connected [Fig. 6(I)], for the undelayed and homogeneously delayed cases, the Lyapunov function between a pair of nodes

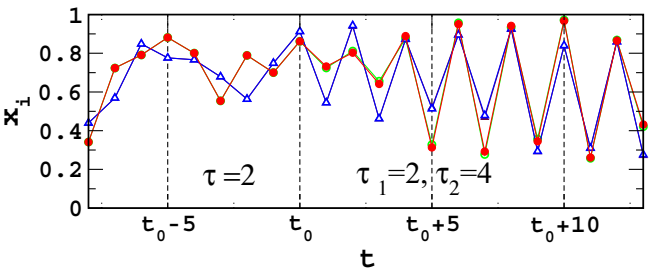

FIG. 5. (Color online) Time evolution of a few nodes in the complete bipartite network of $N = 500$ [the coupling strength is chosen as 0.68 for which the network is shown to form two ideal D clusters for a homogeneous delay ($\tau = 2$) for $t < t_0$]. At $t = t_0$ the heterogeneity in the delay is introduced by randomly making 50% of the connections conducting with $\tau_2 = 4$ and the rest keep on conducting with $\tau_2 = 2$.

becomes

$$V_{12}(t+1) = \{(1-\epsilon)[f(x_1(t)) - f(x_2(t))]\}^2.$$

Thus synchronization between nodes 1 and 2 depends only on the local dynamics of both the nodes and the coupling strength, whereas if nodes in set A are directly connected [Fig. 6(II)] in the Lyapunov function all the coupling terms except the one involving the interaction between 1 and 2 cancel out,

$$V_{12}(t+1) = \Bigg[(1-\epsilon)[f(x_1(t)) - f(x_2(t))] + \frac{\epsilon}{4} g(x_2(t-\tau)) - g(x_1(t-\tau)) \Bigg]^2,$$

thus yielding different criteria for synchronization of these nodes [8].

Next, using the complete bipartite network, we attempt to understand the parity dependence of the mechanism of cluster formation at weak couplings as observed for all the network architectures. A simple analysis of the periodic synchronized state on the complete bipartite networks provides a basic understanding of the different behaviors observed for the lower coupling values. For example, at a weak ε range, the homogeneous delays for $\tau_1 = 1$ manifest the globally synchronized state spanning all the nodes for $0.16 \lesssim \varepsilon \gtrsim 0.2$. The dynamical evolution in this range is periodic with periodicity two, say, $p1$ and $p2$. As heterogeneity in the delay values is introduced

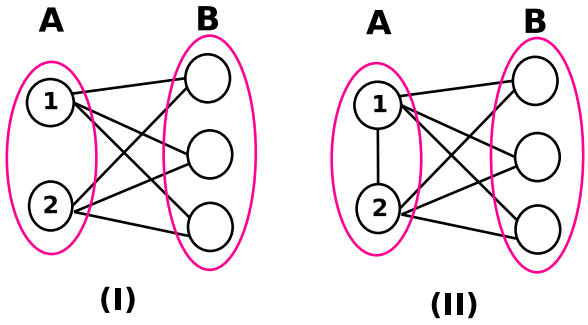

FIG. 6. (Color online) Schematic diagram representing two set of nodes, when a pair of nodes in set A receiving the same inputs are not directly connected (I) and when they are directly connected (II).

such that $f_{\tau_1} = f_{\tau_2} = 0.5$, say, at the $(t+1)$th time step, it leads to the coupling term having a delay part in the evolution equation for the difference variable of the ith and jth nodes as

$$f(x_j(t-\tau_2)) - f(x_i(t-\tau_1)) = \begin{cases} 0 & \text{if } \triangle\tau = 2,4,\ldots, \\ \delta & \text{if } \triangle\tau = 1,3,\ldots, \end{cases}$$

where $\delta = f(p_1) - f(p_2)$ and $\triangle\tau = \tau_2 - \tau_1$. $\triangle\tau$ is even for the odd-odd and the even-even heterogeneity, and odd for the odd-even heterogeneity. Thus the even-even heterogeneity will retain the behavior followed by the even homogeneous delay values, and the odd-odd heterogeneity will retain the behavior followed by the odd homogeneous delay values, whereas the odd-even heterogeneity may disturb the behavior manifested by the even homogeneous or odd homogeneous delays and lead to the mixed cluster state. Note that for diffusive coupling, the odd delays lead to a mismatch in the parity of the delay value of the coupling terms, causing a change in the sign of the coupling term. This may cause a significant impact on the dynamics of the coupled system, leading to different phenomena for the odd and even delays [10,38,39].

Furthermore, we analyze the origin of the mixed and dominant SO clusters for the bipartite networks at intermediate and strong couplings. A closer look into the time evolution of the coupled nodes in the bipartite networks for intermediate ε values reveals that the heterogeneity suppresses the exact synchronization between the nodes which are not directly connected while retaining the phase synchronization between them (see Fig. 5), whereas all the pairs of nodes which are directly connected experience an occurrence of phase synchronization, producing a globally phase synchronized state. In order to further explain the synchronization between the nodes from two different sets at strong couplings, we perform the following analysis. We consider $\varepsilon = 1$, for which all the coupling terms in the difference variable $[x_i(t+1) - x_k(t+1)]$ for a pair of nodes in the same set (i.e., nodes are not directly connected) will get canceled out for the undelayed and the homogeneous delayed cases, causing synchronization of all the pairs of nodes in the set. Let $x_A(t)$ be the synchronized dynamics of nodes in the first set and $x_B(t)$ the synchronized dynamics of the nodes in the second set. For a homogeneous delay ($\tau_{ij} = \tau$), the difference variable for the nodes from the different sets will be

$$x_i(t+1) - x_j(t+1) = g(x_B(t-\tau)) - g(x_A(t-\tau)); \qquad (4)$$

this difference variable will not die for the coupling function $g(x)$ lying in the chaotic regime if the initial conditions for the nodes in the two sets are different. Hence the nodes from different sets do not synchronize, ruling out SO synchronization for the undelayed and homogeneously delayed cases for $\varepsilon = 1$, whereas the heterogeneous delays do not lead to such a simple situation, and the difference variable for the nodes in the different sets takes the form

$$x_i(t+1) - x_k(t+1) = \frac{2}{N}\left[\sum_{i=1}^{N} A_{ik} g(x_k(t-\tau_{ki})) - \sum_{k=1}^{N} A_{ki} g(x_i(t-\tau_{ik}))\right]. \qquad (5)$$

For the heterogeneous delays, the synchronization between a pair of nodes from the same set for $g(x) = 4x(1-x)$ at $\varepsilon = 1$ depends on the coupling from other nodes. Thus, depending on the heterogeneous delay values, these nodes may or may not synchronize. Thus, the presence of heterogeneity in delay breaks the restriction (4) and gives rise to the possibility of synchronization between nodes in different sets. Though the analysis carried out here was done for the extreme coupling value ($\varepsilon = 1$) and cannot be directly applied to other ε values for which another term consisting of the local dynamics of nodes also appears in the difference variable given by Eqs. (4) and (5), at the strong coupling this additional term will have less of an impact on the dynamical evolution as compared to the coupling term, leading to a similar effect being responsible.

V. EFFECT OF THE CHANGE IN AMOUNT OF HETEROGENEITY

So far we have concentrated on the case $h = 1$ corresponding to the maximum heterogeneity. We find that while the amount of heterogeneity plays a crucial role in determining the cluster synchronizability of networks, some cases even demonstrate a transition from no cluster state to all nodes forming clusters [Fig. 7(a)], while the mechanism is still governed by the parity, except for the complete bipartite networks, which show a transition from a robust D cluster state to dominant SO clusters and a single SO cluster state [Fig. 7(b)]. To the end of this section, we provide an understanding of this behavior. Figure 7(a) demonstrates clear examples of the enhancement in the cluster formation while retaining the mechanism in the presence of heterogeneous delays with odd-odd parity. For a homogeneous delay (say, $\tau = 1$), a very smaller number of nodes form clusters (Fig. 7). As some connections start conducting with a different delay value τ_2, there is no significant change in the cluster formation, as depicted in Fig. 7. With a further increase in f_{τ_2}, there is an increment in the number of nodes forming clusters, reaching to all nodes forming clusters for $h \gtrsim 0.4$.

As we have illustrated that the introduction of heterogeneity in delays enhances synchronization and the complete bipartite network already displays 100% nodes participating in the formation of robust D clusters for the homogeneous delay, the only possible way to achieve an enhancement of the synchrony could be via synchronization between nodes of two driven clusters giving rise to SO clusters. The arguments

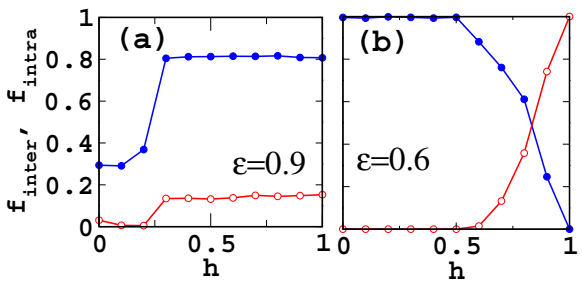

FIG. 7. (Color online) Variation of f_{inter} (solid circles) and f_{intra} (open circles) as a function of the amount of heterogeneity. (a) SF network with $N = 500$ and $\tau_1 = 1, \tau_2 = 3$. (b) The complete bipartite networks with $N = 200$ and $\tau_1 = 2, \tau_2 = 4$. Both graphs are for $f(x) = 4x(1-x)$.

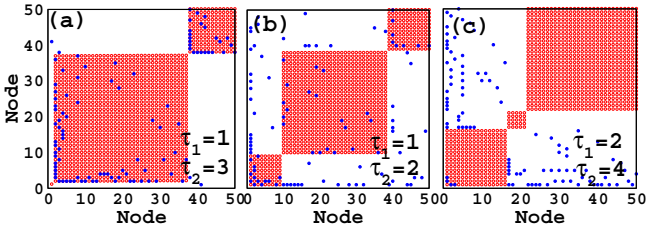

FIG. 8. (Color online) A typical behavior of coupled dynamics illustrating different cluster patterns for changes in the parity of heterogeneous delays. The figure description is the same as in Fig. 3. The example presents a scale-free network with $N = 50$, $\langle k \rangle = 4$, and $\varepsilon = 0.02$. All the graphs correspond to $f_{\tau_1} = f_{\tau_2}$

delivered earlier using a difference variable [Eq. (4)] direct that more heterogeneity in delays will lead to the occurrence of a greater number of pairs of nodes from the same set for which the difference variable does not die, thus destroying synchronization between more pairs of nodes belonging to the same set, and could be a possible reason behind more heterogeneity inducing more SO synchronization.

VI. COUPLED CIRCLE MAPS

In order to demonstrate the robustness of the results, in this section we present results for the coupled circle maps [40]. The local dynamics is given by

$$f(x) = x + \omega + (p/2\pi)\sin(2\pi x)\,(\mathrm{mod}\ 1). \qquad (6)$$

Here we discuss results with the parameters of the circle map in the chaotic region ($\omega = 0.44$ and $p = 6$). As discussed for the logistic map, the coupled circle maps also lead to (i) dependence of the mechanism behind cluster formation on the parity of delays, (ii) the enhancement in the synchronization by introduction of heterogeneity in delays, and (iii) change in the cluster patterns with a change in the heterogeneous delays.

Figure 8 demonstrates the change in the mechanism behind the cluster formation with the change in the parity of the heterogeneous delay values, and exhibits the change in the cluster patterns. These snapshots depict the formation of the SO clusters for odd heterogeneous delays, mixed clusters for the mixed parity of heterogeneous delays, and D clusters for even heterogeneous delays. Figures 9(a) and 9(b) plot examples demonstrating the transition from the ideal D to the globally synchronized state for the coupled circle maps on the complete bipartite networks.

VII. GAUSSIAN DISTRIBUTED DELAYS

In order to see the robustness of the phenomena, such as enhancement in cluster synchronization and a change in the mechanism for the two delay case, we consider the Gaussian distributed delays as [41] $\tau_{ij} = \bar{\tau} + Near(c\eta)$, where η is Gaussian distributed with mean zero and standard deviation one. The delays are homogeneous ($\tau_{ij} = \tau$) for $c = 0$ and are Gaussian distributed around $\bar{\tau}$ for $c \neq 0$. We choose the example of SF networks in order to capture a better overview of the mechanism behind cluster synchronization as they

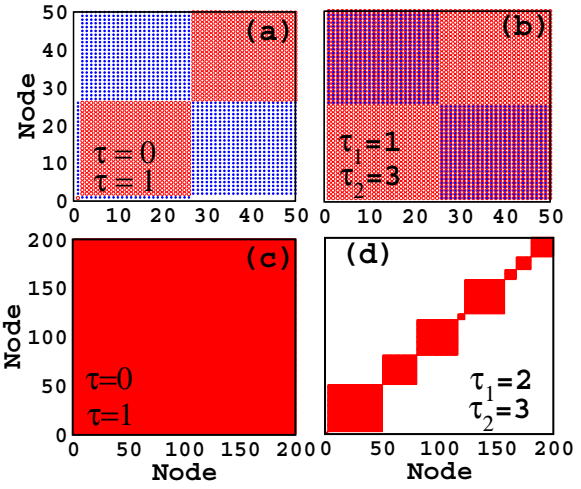

FIG. 9. (Color online) Node vs node diagram demonstrating various cluster states for (a) and (b) for coupled circle maps on complete bipartite networks of $N = 50$ at $\varepsilon = 0.85$, and (c) and (d) for coupled logistic maps on a globally connected network of $N = 200$ at $\varepsilon = 1.0$. (a) and (c) $\tau = 0/\tau = 1$ indicate that exactly the same patterns are obtained for the undelayed ($\tau = 0$) and the homogeneous delayed ($\tau = 1$) cases. Circles and dots remain the same as in Fig. 3. All the graphs correspond to $f_{\tau_1} = f_{\tau_2}$.

are known to exhibit good synchronizability for undelayed and delayed evolution. We find that the distributed delays break the dominance of any of the two mechanisms, clearly visible for the homogeneous and two delay cases, leading to the mixed cluster state for $\varepsilon \gtrsim 0.15$ [Fig. 10(a)]. The other networks we have considered, except for the complete bipartite networks, manifest similar results as for the SF networks. The complete bipartite networks for the Gaussian distributed delays are capable of displaying all the mechanisms of cluster synchronization, as observed for the two delay case [Fig. 10(b)], leading to rich cluster patterns depending on the coupling strength. A comparison with Figs. 2(a) and 2(b) indicates that the Gaussian distributed delays reveals no further phenomena than already observed for the two delay heterogeneity.

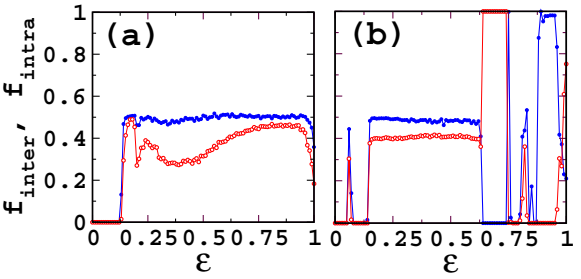

FIG. 10. (Color online) Variation of f_{inter} (solid) and f_{intra} (open) circles as a function of ε for SF (left) and complete bipartite (right) networks with $N = 500$ and for Gaussian distributed delays with mean $\bar{\tau} = 10$ and variance $c = 9$.

VIII. EFFECT OF AVERAGE DEGREE

Previous studies have demonstrated that undelayed and homogeneously delayed evolution of all the networks with a high average degree leads to a globally synchronized state after a critical ε value, whereas the introduction of odd-even heterogeneity leads to the multicluster state. Note that for this multicluster state there is no significant suppression in the overall synchronization in the network, as still almost all (95%) the nodes participate in the cluster formation. The only difference is that the heterogeneity in delays breaks the globally synchronized cluster, distributing its nodes into the different clusters (Fig. 9). The Gaussian distributed delays at strong couplings also generate the multicluster state, as observed for the two delay odd-even heterogeneity.

For the coupled dynamics, there exists a tradeoff between the local dynamics and the coupling term, resulting in various emerging behaviors. At strong coupling values, the coupling term dominates over the local dynamics. Again, as explained earlier, for $\varepsilon = 1$, the Lyapunov function for a pair of nodes [Eq. (2)] in the globally connected networks would depend only on the term $[g(x_j(t-\tau)) - g(x_i(t-\tau))]$ while other terms cancel out, whereas for the heterogeneous delays, the Lyapunov function would contain all the coupling terms (3), thereby making the stability of the synchronized state dependent on the neighbors, and disturbing the synchronization between the nodes for the homogeneous delay case. Therefore, for heterogeneous delays, a pair of nodes i and j may or may not get synchronized depending on the delays connecting to all the neighbors, thereby leading to different cluster patterns such as the multicluster state for a globally coupled network against a global synchronized state for homogeneous delays.

IX. DISCUSSION AND CONCLUSION

We study the impact of heterogeneity in delay values on cluster synchronization and present the results for two different delay arrangements: (i) the heterogeneity with two different delay values, and (ii) the heterogeneity with Gaussian distributed delays. For the first case, the cluster synchronization exhibits a dependence on the amount of heterogeneity in the delays. Our results suggest that the heterogeneous delays accomplish an enhancement in the cluster synchronization for which we provide arguments using simple network structures. The enhancement in cluster synchronization with the enhancement in the heterogeneity in the delays at strong couplings indicates that heterogeneity in the delay may simplify the coupled dynamics.

Next, we find that at weak couplings the different parities impose different constraints on the coupled dynamics, thereby inducing a different mechanism of cluster formation for which we provide an explanation by considering a simple case of periodic evolution. For intermediate and strong couplings, we find that more of the heterogeneity in the delays is associated with enhanced cluster synchronizability of the network. Thus, the amount of heterogeneity can be used as a tool to improve or reduce the cluster synchronizability of the model networks [4,5] and can be used to understand versatile cluster patterns observed in the real world network [23]. The Gaussian distributed delays exhibit similar results as observed for the odd-even delays displaying mixed clusters at weak, intermediate, and strong couplings. All the numerical results indicate that the heterogeneity in delays favor the SO mechanism of synchronization for achieving a better synchrony in the network as connections in the network increase. This is more evident in the case of odd-odd heterogeneity, which advances the ideal D clusters for a network having less connections and manifests a transition to the SO cluster as the connections are increased. Note that for these high average degrees all the networks (except the complete bipartite networks) with homogeneous or zero delay display the globally synchronized state at strong enough coupling strength, while the networks with heterogeneous delays yield the multicluster state, keeping the SO mechanism responsible for the synchronization intact.

Using the Lyapunov function analysis, we furnish the argument that the heterogeneity in delays causes a different coupling environment for nodes that are directly connected, which for the strong coupling regime, where the coupling term dominates over the local evolution, is responsible for disrupting the global cluster. We further substantiate that for the complete bipartite networks, at strong couplings, in the presence of heterogeneity in delays, the combined effect of the two postulates, (i) the destruction of the ideal D cluster state and (ii) the possibility of SO synchronization, leads to the formation of different cluster patterns such as mixed, dominant D, dominant SO, and ideal SO.

To conclude, using extensive numerical simulations for various model networks, accompanied with an analytical understanding using the Lyapunov function for completely bipartite networks, we demonstrate that, in the presence of heterogeneity in delays, the mechanism for cluster synchronization can be completely different from the homogeneous delayed evolution. In the brain, the time of information transmission lies in a range exhibiting a heterogeneity in the time delay [20], and the results presented in this paper can be used to gain insight into the synchronized activities of such systems. Furthermore, the heterogeneous delays have been shown to display regular chaotic patterns in brain networks [42]. Our results may be further extended to study the mechanism behind the origin of these patterns. Furthermore, since our definition of phase synchronization is based on the study of matching local maxima (minima) in the time evolution of the coupled nodes, and recently local maxima (minima) have been found useful in understanding the dynamical behavior of the stock market [43,44], our work may be further extended to investigate the cluster patterns in the stock market.

ACKNOWLEDGMENTS

S.J. acknowledges DST (SR/FTP/PS-067/2011) and CSIR [25(0205)/12/EMR-II] for financial support. A.S. thanks complex systems laboratory members Sanjiv K. Dwivedi, Aparna Rai, and Camellia Sarkar for providing a conducive atmosphere. We thank Jürgen Kurths and C. K. Hu for useful discussions. We acknowledge an anonymous referee for critical remarks which have helped in improving the paper.

[1] B. Blasius, A. Huppert, and L. Stone, Nature (London) **399**, 354 (1999).

[2] A. Schnitzler and J. Gross, Nat. Rev. Neurosci. **6**, 285 (2005).

[3] J. Kestler, W. Kinzel, and I. Kanter, Phys. Rev. E **76**, 035202 (2007).

[4] I. Kanter *et al.*, Europhys. Lett. **93**, 66001 (2011).

[5] A. E. Motter *et al.*, Nat. Phys. **9**, 191 (2013).

[6] S. Jalan and R. E. Amritkar, Phys. Rev. Lett. **90**, 014101 (2003).

[7] S. Jalan, R. E. Amritkar, and C.-K. Hu, Phys. Rev. E **72**, 016211 (2005).

[8] R. E. Amritkar, S. Jalan, and C.-K. Hu, Phys. Rev. E **72**, 016212 (2005).

[9] M. Lakshmanan and D. Senthilkumar, *Dynamics of Nonlinear Time-Delay Systems* (Springer, Berlin, 2010).

[10] F. M. Atay, J. Jost, and A. Wende, Phys. Rev. Lett. **92**, 144101 (2004); F. M. Atay and O. Karabacak, SIAM J. Appl. Dyn. Syst. **5**, 508 (2006); F. M. Atay, Afr. Math. **23**, 109 (2012).

[11] G. C. Sethia, A. Sen, and F. M. Atay, Phys. Rev. Lett. **100**, 144102 (2008).

[12] Y.-H. Shaiv, H.-P. Chiang, Y.-C. Cheng, and C.-K. Hu, J. Phys. Soc. Jpn. **72**, 801 (2003).

[13] T. Dahms, J. Lehnert, and E. Schöll, Phys. Rev. E **86**, 016202 (2012).

[14] A. Singh, S. Jalan, and J. Kurths, Phys. Rev. E **87**, 030902(R) (2013).

[15] A. Singh and S. Jalan, Eur. Phys. J. ST **222**, 885 (2013).

[16] C. R. S. Williams, T. E. Murphy, R. Roy, F. Sorrentino, T. Dahms, and E. Scholl, Phys. Rev. Lett. **110**, 064104 (2013).

[17] W. Kinzel, A. Englert, and I. Kanter, Philos. Trans. R. Soc., A **368**, 379 (2010).

[18] A. Prasad, J. Kurths, and R. Ramaswamy, Phys. Lett. A **372**, 6150 (2008).

[19] J. M. Höfener, G. C. Sethia, and T. Gross, Philos. Trans. R. Soc., A **371**, 1999 (2013).

[20] D. W. Tank and J. J. Hopfield, Proc. Natl. Acad. Sci. USA **84**, 1896 (1987); in *Epilepsy as a Dynamic Disease*, edited by J. Milton and P. Jung (Springer, Berlin, 2003).

[21] J. E. S. Socolar and D. J. Gauthier, Phys. Rev. E **57**, 6589 (1998); M. Rosenblum and A. Pikovsky, *ibid.* **70**, 041904 (2004); A. Ahlborn and U. Parlitz, *ibid.* **75**, 065202 (2007); E. A. Shahverdiev and K. A. Shore, *ibid.* **77**, 057201 (2008); M. Zigzag, M. Butkovski, A. Englert, W. Kinzel, and I. Kanter, *ibid.* **81**, 036215 (2010); F. M. Atay, S. Jalan, and J. Jost, Phys. Lett. A **375**, 130 (2010); C. Masoller and F. Atay, Eur. Phys. J. D **62**, 119 (2011); C. Cakan, J. Lehnert, and E. Schöll, Eur. Phys. J. B **87**, 54 (2014).

[22] R. Szalai and G. Orosz, Phys. Rev. E **88**, 040902(R) (2013).

[23] D. P. Rosin, D. Rontani, D. J. Gauthier, and E. Scholl, Phys. Rev. Lett. **110**, 104102 (2013).

[24] Y. Hong *et al.*, Opt. Lett. **29**, 1215 (2004).

[25] J. Zhou and Z. Liu, Phys. Rev. E **77**, 056213 (2008).

[26] R. Albert and A.-L. Barabasi, Rev. Mod. Phys. **74**, 47 (2002).

[27] K. Kaneko, Phys. Rev. Lett. **63**, 219 (1989).

[28] M. Barahona and L. M. Pecora, Phys. Rev. Lett. **89**, 054101 (2002); P. J. Menck *et al.*, Nat. Phys. **9**, 89 (2013).

[29] A. Pikovsky, M. Rosenblum, and J. Kurths, *Synchronization: A Universal Concept in Nonlinear Sciences* (Cambridge University Press, Cambridge, UK, 2003).

[30] A. Arenas, A. D. Guilera, J. Kurths, Y. Moreno, and C. Zhou, Phys. Rep. **469**, 93 (2008).

[31] S. Boccaletti *et al.*, Phys. Rep. **366**, 1 (2002); S. Boccaletti, in *The Synchronized Dynamics of Complex Systems*, edited by A. C. J. Luo and G. Zaslavsky, Monograph Series on Nonlinear Science and Complexity Vol. 6 (Elsevier, Amsterdam, 2008).

[32] A. Singh and S. Jalan, Physica A **391**, 6655 (2012).

[33] F. S. de San Roman, S. Boccaletti, D. Maza, and H. Mancini, Phys. Rev. Lett. **81**, 3639 (1998).

[34] R. E. Amritkar and S. Jalan, Physica A **346**, 13 (2005).

[35] S. Wiggins, *Introduction to Applied Nonlinear Dynamical Systems and Chaos* (Springer, Berlin, 1990); R. He and P. G. Vaidya, Phys. Rev. A **46**, 7387 (1992).

[36] S. Acharya and R. E. Amritkar, Europhys. Lett. **99**, 40005 (2012).

[37] P. Ashwin, J. Buescu, and I. Stewart, Phys. Lett. A **193**, 126 (1994); S. C. Venkataramani, B. R. Hunt, and E. Ott, Phys. Rev. E **54**, 1346 (1996).

[38] R. Cheng *et al.*, Chaos **23**, 043108 (2013).

[39] T. Buchner and J. J. Zębrowski, Phys. Rev. E **63**, 016210 (2000); R. C. Penner, *Discrete Mathematics: Proof Techniques and Mathematical Structures* (World Scientific, Singapore, 1999).

[40] S. J. Shenker, Physica D **5**, 405 (1982).

[41] C. Masöller and A. C. Marti, Phys. Rev. Lett. **94**, 134102 (2005).

[42] M. Pais-Vieira *et al.*, Sci. Rep. **3**, 1319 (2013); G. Dumas *et al.*, PLoS ONE **5**, 12166 (2010); H. Braak *et al.*, J. Neural Transm. **103**, 455 (1996).

[43] A. Grönlund, II. Gu. Yi, and B. J. Kim, PLoS ONE **7**, e33960 (2012).

[44] F. Garzarelli *et al.*, Sci. Rep. **4**, 4487 (2014).